LINEAR STABILITY THEORY APPLIED IN A CROSS-STREAM PROFILE OF A SHEAR LAYER OF A LEADING EDGE SLAT

Fernando H T Himeno

Filipe R do Amaral

Marcello A F de Medeiros

fernando.himeno@gmail.com

framaral@usp.br

marcello@sc.usp.br

Sao Carlos Engineering School, University of Sao Paulo

Trabalhador Sao Carlense Avenue, 400. Zip-Code 13566-590. Sao Carlos, Sao Paulo, Brazil.

Abstract. *Aircraft noise has been a topic of interest in aeronautics since 70s. A large portion of noise was reduced with the inclusion of turbofan engines and then intense efforts were dedicated to the reduction of airframe noise in which high-lift surfaces represent one of the most critical sources. Leading edge slat, employed in a large part of the air fleet in most of the large aircrafts, is a high-lift system distributed over the whole wing span and this increases its importance in noise studies. The shear layer flow in the slat cove is very turbulent and is the source of the slat noise. In order to understand the shear layer features and fluctuations related to structures that could be related to sources of noise, a numerical study is presented. Linear Stability Theory was applied to the mean flow of the slat cove shear layer. Cross-stream profiles were approximated to hyperbolic tangent functions. Results of most unstable frequencies and amplitudes of fluctuation velocity along the shear layer shows good agreement with experimental data.*

Keywords: *Aeroanautics, Aeroacoustics, Slat, LST*

Introduction

High-lift devices, namely slat and flap, aim at increasing the wing lift coefficient, therefore it became possible for the aircraft to take of in shorter runways and to land at a lower speed. Hence, both procedures became safer and the aircraft is able to operate in a wide range of airports. On the other hand, the deployed high-lift devices may increase the aeroacoustic noise emissions by as much as 10 dB in comparison with the same wing operating at stowed configuration (Dobrzynski, 2010).

The slat device shows a lower intensity per unit area noise source than the flap tip source. However, as the slat is an element extended over the whole wing span, hence its noise source, whereas the flap tip is a much more localized noise source in the aircraft wings. For aircraft category of regional routes, the ratio between the wing span and the other airframe components, e.g., landing gears and fuselage, is higher than that observed for larger aircraft categories. Hence, the understanding of slat noise generation mechanisms for regional routes aircraft is of paramount importance if one aims at develop noise reduction strategies.

The noise spectra of a two-dimensional, unswept and untappered slat is commonly divided into three main components, i.e., the low-frequency narrowband peaks, the mid-frequency broadband and the high-frequency hump components (Imamura et al., 2009; Amaral et al., 2016).

The low-frequency narrowband peaks is the most controversial component, as studies suggest it owe the small scale models, and hence the lower *Reynolds* numbers, experimented in wind-tunnels (Dobrzynski, 2010). In order to suppress such narrowband peaks, some attempts at forcing the boundary-layer transition upstream the slat cusp lower surface succeed (Dobrzynski et al., 2008; Dobrzynski and Pott-Pollenske, 2001), although not all of them achieved success (Kolb et al., 2007; Imamura et al., 2009; Murayama et al., 2014). Several investigations points to an acoustic feedback mechanism, the so-called *Rossiter* modes (Rossiter, 1964), as the responsible for the narrowband peaks (Roger and Perennes, 2000; Kolb et al., 2007; Terracol et al., 2011; Manoha et al., 2012; Pascioni et al., 2014). Numerical simulations results in combination with the *Proper Orthogonal Decomposition* (*POD*) technique (Souza et al., 2013, 2015), associated the far-field narrowband peaks with *Kelvin-Helmholtz* vortices in the slat cove mixing layer.

The broadband slat noise component is usually assumed as the primary slat noise source, although its noise generation mechanism still not completely understood. Computational simulations conducted by Pott-Pollenske, Alvarez-Gonzalez and Dobrzynski (2003)(Pott-Pollenske et al., 2003) suggested the slat broadband noise is a consequence of the turbulent flow originated in the mixing layer reattachment point at the slat cove and convected through the slat gap. Lockard and Choudhari (2011)(Lockard and Choudhari, 2011) numerically investigated the noise from the *MD30P30N*, varying the *Mach* and *Reynolds* numbers. They achieved a good data collapse with the $5th$ *Mach* power law - a similar scaling is observed for experimental results (Dobrzynski and Pott-Pollenske, 2001; Mendoza et al., 2002; Guo et al., 2003; Murayama et al., 2014) - and found the *Reynolds* number varying produced almost no impact on the slat noise spectra.

The high-frequency hump component is related to the vortex shedding from the slat trailing-edge, as demonstrated by several experiments and numerical simulations (Khorrami et al., 2000; Choudhari et al., 2002; Mendoza et al., 2002). Dobrzynski (2010)(Dobrzynski, 2010) indicates the vortex shedding from the slat trailing-edge is usually observed in two-dimensional scaled models and such a phenomenon is different from that observed for full-size aircraft, as for models the ratio between the slat trailing-edge thickness and the slat chord is much higher than for full-size aircraft, i.e., the airfoil models exhibit a blunt slat trailing-edge.

Most part of the studies on slat noise employ idealized high-lift geometries (Jenkins et al., 2004; Lockard and Choudhari, 2009; Manoha et al., 2012; Pagani et al., 2016), with no elements necessary for enabling the slat operation, such as the ones present on the slat cove, e.g., deflection mechanisms, deicing systems and the sealing devices employed for the avoidance of flow in the gap between the slat and the main element under cruise conditions. Recently, the assessment of the aeroacoustic impact of such devices have drawn the attention of the research community. Numerical simulations on slat cove bulb seals, (Khorrami and Lockard, 2010; Bandle et al., 2012; Souza et al., 2015), showed the seal may increase in the amplitude of the slat noise spectra low-frequency narrowband peaks component. Nevertheless, experiments with a slat cove filler fairing (Kolb et al., 2007) and even with bulb seals (Amaral et al., 2015) showed the seals have a narrowband peaks slat noise component suppression potential.

This paper aims at explore the slat cove shear layer features and fluctuations which may be related to noise sources for a slat of an *MD30P30N* airfoil profile. Numerical simulations were conducted and the *Linear Stability Theory* was applied on the slat cove shear layer mean flow, with the cross-stream profiles approximated to hyperbolic tangent functions.

Methodology

Simulations using commercial code PowerFLOW were conducted for some experimental cases varying seal positions in the slat cove surface. The software showed good results on study of problems involving aerocoustics as presented in earlier works (Lafitte and Perot, 2009; Souza et al., 2013, 2015; Pagani et al., 2016). Based on Laticce-Boltzmann Method, it solves the discrete Boltzmann (Equation 1), through the approximation given by Bhatnagar et al. (1954). This equation represents the probability of find a particle at some position and velocity considering the momentum exchange between others particles, where f_i is the probability density function and τ, relaxation time.

$$f_i(\vec{x} + \epsilon_i \Delta t, t + \Delta t) = f_i(\vec{x}, t) + \frac{\Delta t}{\tau}[f_i^{eq}(\vec{x}, t) - f_i(\vec{x}, t)]. \tag{1}$$

Ffowcs Williams-Hawkings analogy is applied to calculate the farfield propagated noise based on nearfield data. The turbulence model $RNG\ k - \epsilon$ are used to solve the smallest turbulent scales and the boundary condition are applied at the finite volumes adjacent to the walls. The inflow considered Dirichlet condition with horizontal velocity of $U_\infty = 34\ m/s$ and outflow Neumann condition fixing pressure at $1\ atm$. Simulations also considered Mach number of 0.1 and Reynolds number of 10^6 to reproduce experiment setup. Turbulence level considered 0.09% the ratio between velocity fluctuation and U_∞.

A cartesian mesh were implemented, in order to facilitate the inclusion of complex geometries, and it is finer at regions close to the airfoil. Domain and mesh independence tests were also conducted and results could be found in previous works showing mesh independence studies even for cases including a small excrescence on the slat cove wall (Simões et al., 2011;

Souza, 2012). Domain height were $1.7\ m$ and in streamwise direction and such a length were chosen after domain independence tests. The finest volume edge had $0.2\ mm$ close to airfoil surface and slat cove. Slat geometry also presents a blunt trailing edge corresponding to 0.092% of airfoil stowed chord. Nevertheless, the mesh refinement around the slat trailing edge were not sufficient to properly solve the vortex shedding present at this region.

The airfoil geometry corresponds to MD30P30N with slat modified with inclusion of a excrescence attached on its cove. This case represents a more realistic situation, where mechanical insulation seal is used inside cove to avoid surface contact between slat and main element surfaces. Figure 1 schematizes the airfoil and slat cove seal, where d is measured from trailing edge and is non-dimensionalized by slat chord.

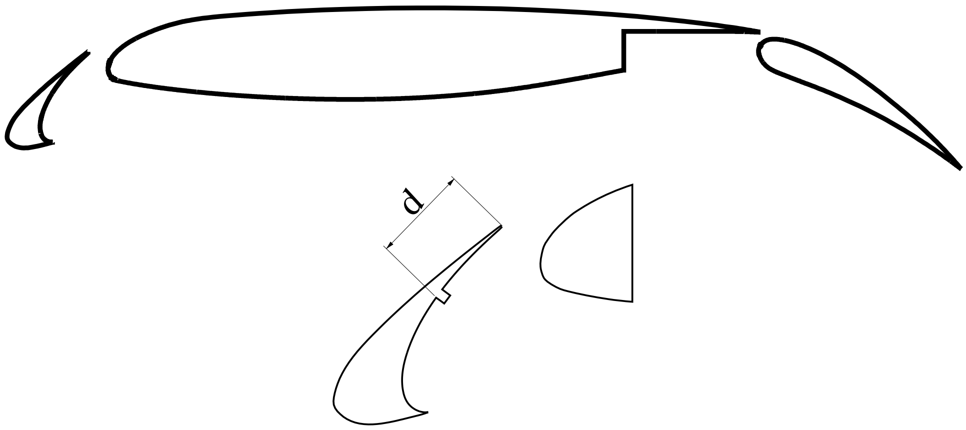

Figure 1: MD30P30N geometry and detail of slat cove seal attached on its surface. $d = 0.41$ **is non-dimensionalized by the slat chord.**

The stability theory of small pertubations considers the stream function

$$\Psi(x, y, t) = \phi(y)e^{i\alpha(x-ct)}, \tag{2}$$

where the flow is considered parallel, α, the wavenumber, c, the phase velocity and ω, the frequency. The eingenfunctions are derived relating ϕ function with the shape of streamwise and cross-stream velocity. Hence, the Rayleigh equation (Eq.(3)) is derived from Navier-Stokes with parallel flow condition considered.

$$[U^*(y^*; \lambda) - c](\phi" - \alpha^2\phi) - U^{*}"(y; \lambda)\phi = 0. \tag{3}$$

Mean velocity profile, U, were approximated to a tanh profile by Monkewitz and Huerre (1982); Huerre and Monkewitz (1990). Then a function for cross-stream velocity could be given by

$$U^*(y^*) = (\Delta U/2)tanh(2y^*/\delta_\omega) + \overline{U}, \tag{4}$$

where y^* is the cross-stream coordinate, ΔU is the difference of maximum and minimum velocity, $\overline{U}$ is the velocity average and $\delta_\omega = \Delta U^*/(\frac{dU}{dy^*})_{max}$ is the vorticity thickness. Numerical results used here are shown by Monkewitz and Huerre (1982) and Figure 2 shows the amplification rate and most unstable frequencies in function of λ parameter.

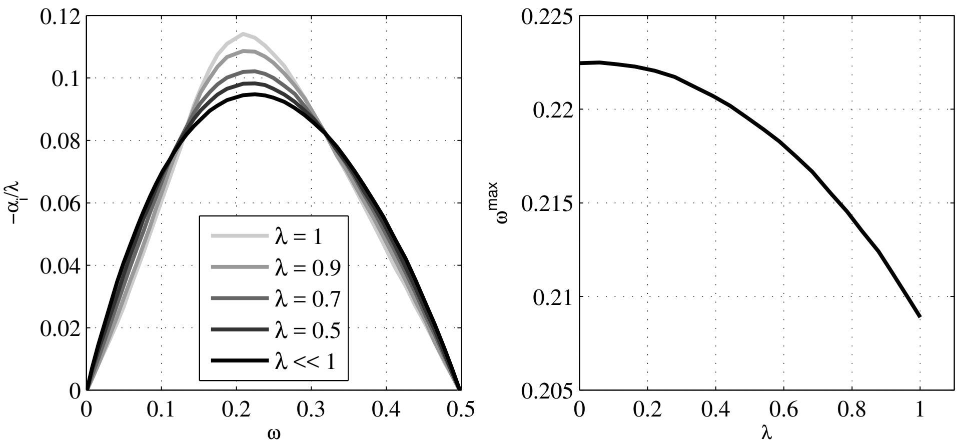

Figure 2: Amplification rate and most unstable frequency shown by Monkewitz and Huerre (1982) in function of $\lambda = \Delta U/2\overline{U}$ parameter. The non-dimensionalization is given by $\overline{U}$ and $\frac{\delta_\omega}{4}$ (momentum thickness).

Results

Figure 3 shows the mean flow streamlines and resolved Turbulent Kinect Energy for baseline (with no seal) and sealed cases for $d = 0.23$, 0.41 and 0.60 positions. The main difference among baseline and sealed cases is the additional recirculation region given by the seal inclusion. TKE shows the turbulence of the sealed cases was not concentrated in the reattachment point, as in baseline, althought it was also spread along shear layer.

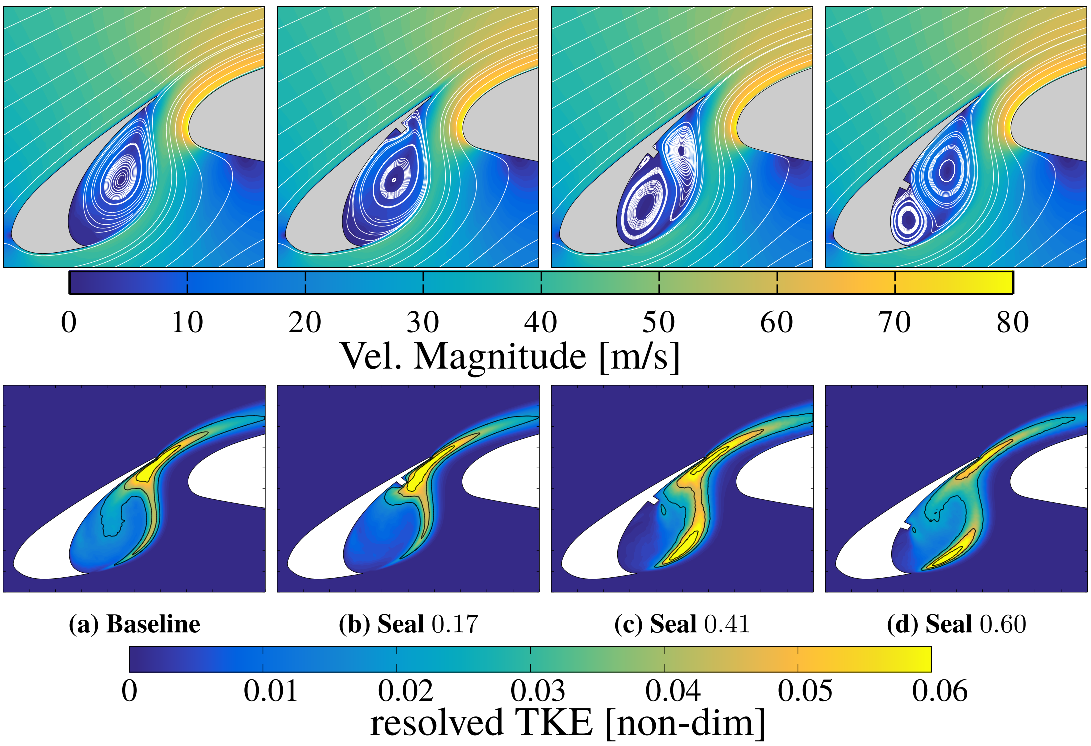

Figure 3: Streamlines and resolved TKE for baseline and sealed cases. 34 **m/s** U_∞**; Angle of attack** $3°$**.**

The cross-stream velocity profiles along the shear layer are shown in Fig. 4, where the full line corresponds to the simulation results and the dashed line corresponds to a hyperbolic tangent function given by Eq. 4. The vorticity thickness of each stage were calculated using numerical data through expression $\delta_\omega = \Delta U^*/(\frac{dU}{dy^*})_{max}$. The positions displayed in the figure correspond to 45 %, 60 % and 81 % of the total shear layer length (cusp to reattachment point) and good approximations were observed.

The evolution of δ_ω along the mixing layer is shown in Fig. 5. The regions where the variable $\lambda = (\Delta U/2\overline{U})$, the one that represents the velocity difference across tanh profile, is higher than 1.3. This represent a situation where the LST predicts absolute instability as discussed by Huerre and Monkewitz (1990). For this reason only the region displayed in full line is used for the analysis of the shear layer most unstable frequency that follows. Despite of that, this plot shows that sealed cases at positions 0.41 and 0.60 have a thicker vorticity thickness compared to baseline, as expected from TKE results.

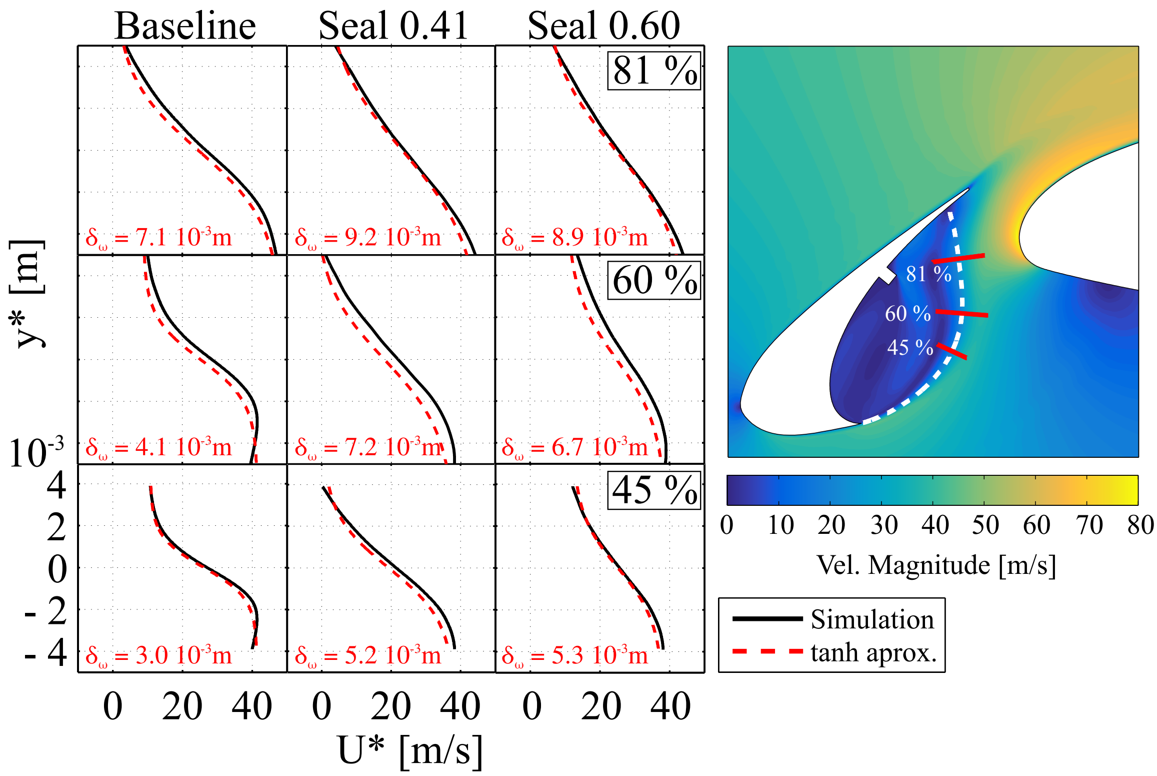

Figure 4: Velocity Magnitude plot with dividing streamline (black). Cross-stream considered for LST are presented in points 12%, 20%, 45%, 60% and 81% of shear layer (white). 34 m/s U_∞; $3°$.

Power Spectrum Density (PSD) of the streamwise velocity fluctuations are plotted in Fig. 6 taking into account the center half points of domain in the spanwise direction. Time series were divided in blocks with 50% of overlap and a Hanning filter was then applied. The results for baseline and seal at positions 0.23 cases follows the same tendency as expected from streamlines and TKE field, where only one recirculation region are present and the turbulent region concentrates in reattachment point. For those cases, the velocity fluctuation develops from high to low frequency along the shear layer. For the sealed case at position 0.60, such a tendency is not observed and the fluctuation level remains almost at same intensity since the cusp to the reattachment point.

LST was employed to predict the most unstable frequency and amplitude development through results presented in Fig. 2. Similar investigation was done by (Deck and Laraufie, 2013)

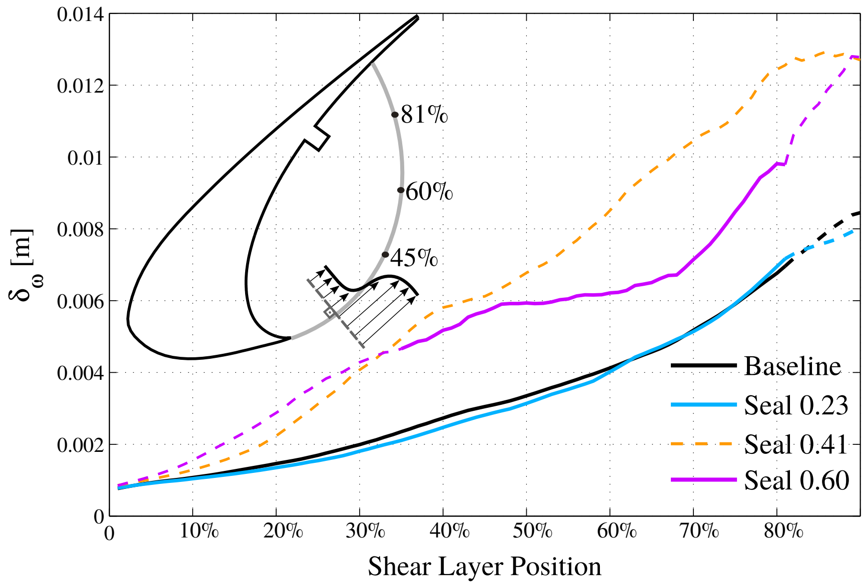

Figure 5: Vorticity thickness evolution considering tanh profile in cross-stream direction.

and showed good agreement, althought only for the initial stages of the baseline geometry shear layer. The fluctuation amplitude was calculated through Eq. 5 considering constant fluctuation level along all frequencies (red dashed line). The most unstables frequencies (ω^{max}) are also exhibited (vertical dashed line). For baseline and seal 0.23, the initial position considered for integration was 20% of shear layer for the case with the seal 0.60, such a position was 35%. The reason for the difference among the cases was the prediction of absolute instability due to the presence of second recirculation region in the region near to the slat cusp.

$$A(\omega; x_{SL}) = A_0(\omega; x_0)\, e^{\int_{x_0}^{x_{SL}} -\alpha_i(\omega; x_{SL})\, dx_{SL}}. \qquad (5)$$

Conclusions

This study attempted to apply the LST to a slat shear layer with baseline and sealed geometries. This analysis could predict the most unstables modes of the mixing layer that could be related to sound generation inside the cove flow. Results show vorticity thickness increases with the presence of a cove excrescence at some positions due mainly to the additional recirculation region created by the interaction of cove flow and seal edges. This represent more complex phenomena due to additional vortical structures interacting with the shear layer. For this reason some regions of shear layer of the sealed cases with two recirculation regions could not be fully analyzed by LST. For baseline and sealed geometries where only a recirculation region is present, the LST could be employed used to predict the development of broadband velocity fluctuation. The most unstable frequency (ω^{max}) develops from higher to lower frequency and this could be the mechanism of increasing the peaks in the spectrum, observed in Fig. 6. Future work will concentrate in the application of LST in geometries of slat with no seal, varying gap, overlap and angle of attack. This approach intends the better understanding of the spectrum narrowband peaks mechanism and its dependency with shear layer parameters.

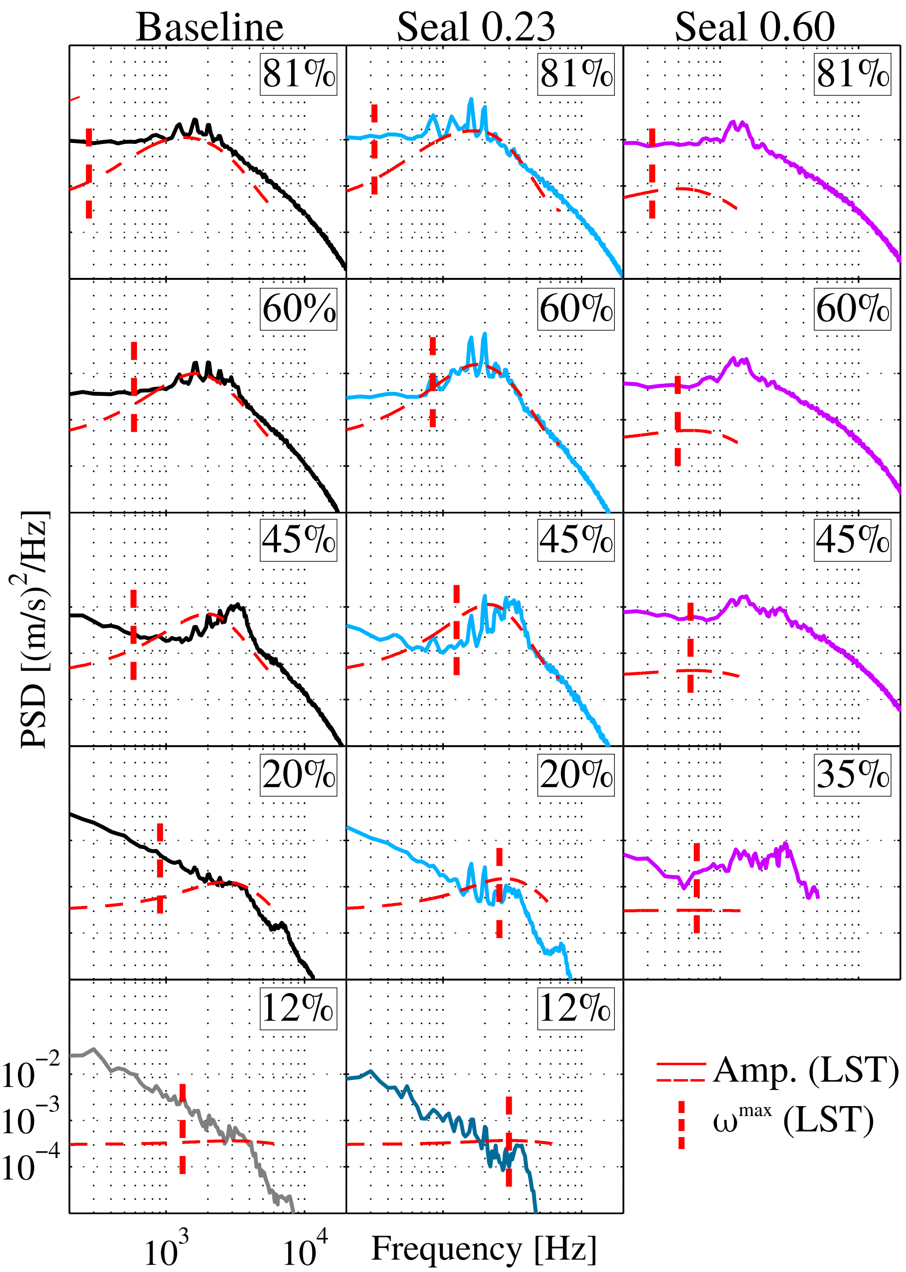

Figure 6: PSD of Streamwise Velocity Fluctuation development along Shear Layer for numerical and LST amplitude prediction. Initial position for amplitude calculation was 12% **(baseline and seal** 0.23**) and** 35% **(seal** 0.60**).**

ACKNOWLEDGEMENTS

Himeno F.H.T, Amaral F.R. and Medeiros M.A.F. received funding from Sao Paulo Research Foundation (FAPESP/Brazil - grant #2016/02970-5), Coordination for the Improvement of Higher Education Personnel (CAPES/Brazil - grant #DS00011/07-0) and CNPq/Brazil (grant #304243/2013-2), respectively.

References

Amaral, F. R., Souza, D. S., Pagani, Jr, C. d. C., Himeno, F. H. T., and Medeiros, M. A. F. (2015). Experimental study of the effect of a small 2d excrescence placed on the slat cove surface of an airfoil on its acoustic noise. In *21st AIAA/CEAS Aeroacoustics Conference*, page 3138. American Institute of Aeronautics and Astronautics.

Amaral, F. R. d., Himeno, F. H. T., Pagani, Jr, C. d. C., and Medeiros, M. A. F. (2016). Experiments on slat noise from -6 to 18 degrees angles of attack. In *46th AIAA Fluid Dynamics Conference*, page 3629. American Institute of Aeronautics and Astronautics.

Bandle, L., Souza, D., Simões, L., and Medeiros, M. (2012). On detrimental effects of excrescences on the slat noise. In *18th AIAA/CEAS Aeroacoustics Conference (33rd AIAA Aeroacoustics Conference)*, page 2099. American Institute of Aeronautics and Astronautics.

Bhatnagar, P. L., Gross, E. P., and Krook, M. (1954). A model for collision processes in gases. i. small amplitude processes in charged and neutral one-component systems. *Physical Review*, 94(3):511–525.

Choudhari, M. M., Lockard, D. P., Macaraeg, M. G., Singer, B. A., Streett, C. L., Neubert, G. R., Stoker, R. W., Underbrink, J. R., Berkman, M. E., and Khorrami, M. R. (2002). Aeroacoustic experiments in the langley low-turbulence pressure tunnel. *NASA TM*, 211432:1–46.

Deck, S. and Laraufie, R. (2013). Numerical investigation of the flow dynamics past a three-element aerofoil. *Journal of Fluid Mechanics*, 732:401–444.

Dobrzynski, W. (2010). Almost 40 years of airframe noise research: What did we achieve? *Journal of Aircraft*, 47(2):353–367.

Dobrzynski, W., Ewert, R., Pott-Pollenske, M., Herr, M., and Delfs, J. (2008). Research at dlr towards airframe noise prediction and reduction. *Aerospace Science and Technology*, 12(1):80–90.

Dobrzynski, W. and Pott-Pollenske, M. (2001). Slat noise source studies for farfield noise prediction. In *7th AIAA/CEAS Aeroacoustics Conference and Exhibit*, page 2158. American Institute of Aeronautics and Astronautics.

Guo, Y., Yamamoto, K., and Stoker, R. (2003). Component-based empirical model for high-lift system noise prediction. *Journal of Aircraft*, 40(5):914–922.

Huerre, P. and Monkewitz, P. A. (1990). Local and global instabilities in spatially developing flows. *Annual review of fluid mechanics*, 22(1):473–537.

Imamura, T., Ura, H., Yokokawa, Y., and Yamamoto, K. (2009). A far-field noise and near-field unsteadiness of a simplified high-lift-configuration model (slat). In *47th AIAA Aerospace Sciences Meeting including The New Horizons Forum and Aerospace Exposition*, page 1239. American Institute of Aeronautics and Astronautics.

Jenkins, L., Khorrami, M., and Choudhari, M. (2004). Characterization of unsteady flow structures near leading-edge slat: Part i: Piv measurements. In *10th AIAA/CEAS Aeroacoustics Conference*, page 2801. American Institute of Aeronautics and Astronautics.

Khorrami, M. R., Berkman, M. E., and Choudhari, M. (2000). Unsteady flow computations of a slat with a blunt trailing edge. *AIAA Journal*, 38(11):2050–2058.

Khorrami, M. R. and Lockard, D. P. (2010). Effects of geometric details on slat noise generation and propagation. *International Journal of aeroacoustics*, 9(4):655–678.

Kolb, A., Faulhaber, P., Drobietz, R., and Grünewald, M. (2007). Aeroacoustic wind tunnel measurements on a 2d high-lift configuration. In *13th AIAA/CEAS Aeroacoustics Conference (28th AIAA Aeroacoustics Conference)*, page 3447. American Institute of Aeronautics and Astronautics.

Lafitte, A. and Perot, F. (2009). Investigation of the noise generated by cylinder flows using a direct lattice-boltzmann approach. In *15th AIAA/CEAS Aeroacoustics Conference (30th AIAA Aeroacoustics Conference)*, page 3268.

Lockard, D. P. and Choudhari, M. (2009). Noise radiation from a leading-edge slat. In *15th AIAA/CEAS Aeroacoustics Conference (30th AIAA Aeroacoustics Conference)*, page 3101. American Institute of Aeronautics and Astronautics.

Lockard, D. P. and Choudhari, M. (2011). The variation of slat noise with mach and reynolds numbers. In *17th AIAA/CEAS Aeroacoustics Conference (32nd AIAA Aeroacoustics Conference)*, page 2910. American Institute of Aeronautics and Astronautics.

Manoha, E., Terracol, M., Lemoine, B., Griffon, L., and Garrec, L. (2012). Slat noise measurement and numerical prediction in the valiant programme. In *18th AIAA/CEAS Aeroacoustics Conference (33rd AIAA Aeroacoustics Conference)*, page 2100. American Institute of Aeronautics and Astronautics.

Mendoza, J., Brooks, T., and Humphreys, W. (2002). Aeroacoustic measurements of a wing/slat model. In *8th AIAA/CEAS Aeroacoustics Conference & Exhibit*, page 2604. American Institute of Aeronautics and Astronautics.

Monkewitz, P. A. and Huerre, P. (1982). Influence of the velocity ratio on the spatial instability of mixing layers. *The Physics of Fluids*, 25(7):1137–1143.

Murayama, M., Nakakita, K., Yamamoto, K., Ura, H., Ito, Y., and Choudhari, M. M. (2014). Experimental study on slat noise from 30p30n three-element high-lift airfoil at jaxa hard-wall lowspeed wind tunnel. In *20th AIAA/CEAS Aeroacoustics Conference*, AIAA Aviation, page 2080. American Institute of Aeronautics and Astronautics. doi:10.2514/6.2014-2080.

Pagani, Jr., C. d. C., Souza, D. S., and Medeiros, M. A. F. (2016). Slat noise: Aeroacoustic beamforming in closed-section wind tunnel with numerical comparison. *AIAA Journal*, 54(7):2100–2115.

Pascioni, K., Cattafesta, L. N., and Choudhari, M. M. (2014). An experimental investigation of the 30p30n multi-element high-lift airfoil. In *20th AIAA/CEAS Aeroacoustics Conference*, AIAA Aviation, page 3062. American Institute of Aeronautics and Astronautics. doi:10.2514/6.2014-3062.

Pott-Pollenske, M., Alvarez-Gonzalez, J., and Dobrzynski, W. (2003). Effect of slat gap/overlap on farfield radiated noise. In *9th AIAA/CEAS Aeroacoustics Conference and Exhibit*, page 3228. American Institute of Aeronautics and Astronautics.

Roger, M. and Perennes, S. (2000). Low-frequency noise sources in two-dimensional high-lift devices. In *6th Aeroacoustics Conference and Exhibit*, Aeroacoustics Conferences, page 1972. American Institute of Aeronautics and Astronautics. doi:10.2514/6.2000-1972.

Rossiter, J. E. (1964). Wind-tunnel experiments on the flow over rectangular cavities at subsonic and transonic speeds. Report, Ministry of Aviation; Royal Aircraft Establishment; RAE Farnborough.

Simões, L., Souza, D., and Medeiros, M. (2011). On the small effect of boundary layer thicknesses on slat noise. In *17th AIAA/CEAS Aeroacoustics Conference (32nd AIAA Aeroacoustics Conference)*, page 2906. American Institute of Aeronautics and Astronautics.

Souza, D., Rodriguez, D., Simoes, L., and Medeiros, M. (2015). Effect of an excrescence in the slat cove: Flow-field, acoustic radiation and coherent structures. *Aerospace Science and Technology*, 44:108–115. Instability and Control of Massively Separated Flows.

Souza, D. S. (2012). *Simulação numérica de ruído de eslate em configuraçõs práticas usando um código comercial*. Thesis.

Souza, D. S., Rodriguez, D., and Medeiros, M. A. F. (2013). A study of the sources of slat noise using proper orthogonal decomposition. In *19th AIAA/CEAS Aeroacoustics Conference*, page 2163. American Institute of Aeronautics and Astronautics.

Terracol, M., Manoha, E., and Lemoine, B. (2011). Investigation of the unsteady flow and noise sources generation in a slat cove: hybrid zonal rans/les simulation and dedicated experiment. In *20th AIAA Computational Fluid Dynamics Conference*, page 3203. American Institute of Aeronautics and Astronautics.